Crystallization Rate Minima in a Series of *n*-Alkanes from $C_{194}H_{390}$ to $C_{294}H_{590}$

E. Boda and G. Ungar*

Department of Engineering Materials, University of Sheffield, Sheffield S1 3JD, U.K.

G. M. Brooke, S. Burnett, S. Mohammed, and D. Proctor

Chemistry Department, Science Laboratories, University of Durham, South Road, Durham DH1 3LE, U.K.

M. C. Whiting

School of Chemistry, University of Bristol, Cantock Close, Bristol 8, U.K.

Received October 29, 1996

ABSTRACT: Melt-crystallization kinetics of long monodisperse *n*-alkanes with chain lengths in the region between 194 and 294 C atoms was investigated by differential scanning calorimetry (DSC) and real-time small-angle X-ray diffraction. Isothermal crystallization experiments on $C_{294}H_{590}$ and cooling experiments on $C_{194}H_{390}$, $C_{198}H_{398}$, $C_{210}H_{422}$, $C_{246}H_{494}$, and $C_{258}H_{518}$ confirmed that in all cases the crystallization rate reaches a maximum several degrees below the melting point of the extended-chain crystal form, followed by a minimum as crystallization temperature is lowered by a further few degrees. This anomalous rate effect has been observed previously for melt-crystallization of $C_{246}H_{494}$ and $C_{198}H_{398}$, and also for solution-crystallization of $C_{198}H_{398}$. The effect is interpreted in terms of "self-poisoning" of the crystal growth surface, i.e. obstruction to chain extension by frequent deposition of the nearly-stable chain-folded overgrowth. The present results confirm the generality of this process which, it is believed, also operates in crystallization of polydisperse polymers.

Introduction

Normal alkanes of strictly uniform chain lengths in the range of several hundred C atoms[1,2] are invaluable models in studying polymer crystallization and morphology.[3−5] Alkanes in the region of 150 C atoms can already form chain-folded crystals, and the longest alkane synthesised so far, $C_{390}H_{782}$, could be solution-crystallized with chains folded in five. There is a marked preference for "integer folding", whereby the fold length adopts values $l \simeq L/n$, with L being the extended chain length and n an integer.

One of the most intriguing findings of the research on long alkanes is the anomalous dependence of crystallization rate on crystallization temperature T_c found for alkanes $C_{198}H_{398}$ and $C_{246}H_{494}$.[6,7] At small supercoolings ΔT of the melt or solution the crystallization rate first increases with increasing ΔT, as expected. However, as ΔT exceeds several degrees, crystallization rate reaches a maximum and then starts to *decrease*. A minimum in crystallization rate occurs at a temperature T^*, below which the rate increases steeply with further increase in ΔT. Real-time small-angle X-ray scattering (SAXS) experiments revealed that the minimum occurs at the transition between the extended-chain and folded-chain crystallization.[6] More recently, linear growth rates and primary nucleation rates have been measured separately for melt crystallization,[8] and both were shown to display a minimum as a function of ΔT.

At the time reservations were expressed in the literature as to the generality of these rate effects. Mandelkern et al.,[9] using alkanes which were prepared by Lee and Wegner via a different synthetic route,[2] reported that they had not observed crystallization rate minima in $C_{168}H_{338}$, $C_{192}H_{386}$, and $C_{240}H_{482}$. The new synthesis at Durham[10] resulted in alkanes of a number of different chain lengths, enabling us to test the generality of the rate anomalies observed previously. Here we report DSC results confirming the existence of the rate minimum in all six available *n*-alkanes in the range between 194 and 294 C atoms.

Table 1. Melting Temperatures of Extended-Chain Crystals of *n*-Alkanes Used in This Study

alkane	T_m (°C)
$C_{194}H_{390}$	126.9
$C_{198}H_{398}$	127.0
$C_{210}H_{422}$	127.4
$C_{246}H_{494}$	128.6
$C_{258}H_{518}$	128.8
$C_{294}H_{590}$	129.5

Experimental Section

The syntheses of all the straight chain paraffins used in this work have been described in ref 10.

DSC experiments were carried out with a Perkin-Elmer DSC-7 instrument. For isothermal and cooling experiments, temperature correction was determined by linear extrapolation to zero and negative heating rates of the calibration error recorded for a range of positive heating rates between 0.5 and 40 K/min, using indium as a standard. Sample weights in the range of 1 mg were used for cooling experiments and 4 mg for isothermal experiments on $C_{294}H_{590}$.

Melting points of extended-chain crystals of *n*-alkanes used in this work are listed in Table 1. Prior to melting point determination, the samples were melt-crystallized directly in the extended-chain form and subsequently annealed below the melting point. Increasing annealing times were used with increasing chain length.

Real-time small-angle X-ray diffraction (SAXS) experiments were carried out on Stations 8.2 and 2.1 of the Synchrotron Radiation Source at Daresbury. The beam was double focused on a Daresbury quadrant multiwire detector at a 4 m distance from the sample. The beam cross-section was 1.5 × 0.3 mm at the specimen which was held in a thin-walled borosilicate glass capillary in a customized Linkam heating/cooling stage. Analog output from a separate thermocouple touching the

* Author for correspondence.

⊗ Abstract published in *Advance ACS Abstracts,* July 1, 1997.

S0024-9297(96)01599-9 CCC: $14.00

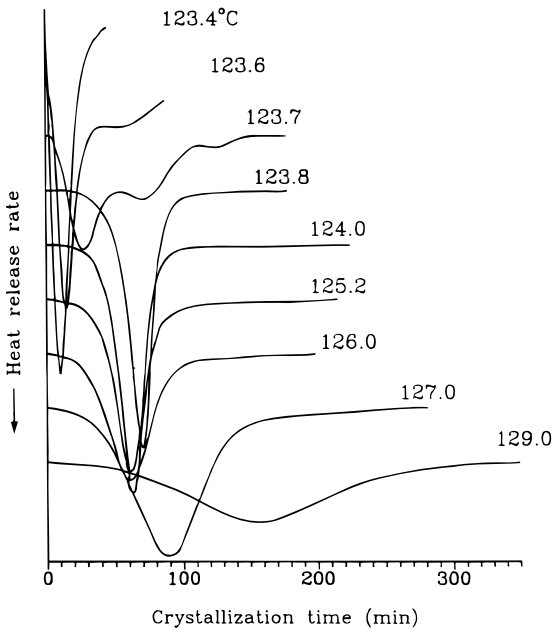

Figure 1. Isothermal crystallization exotherms recorded by DSC for *n*-alkane $C_{294}H_{590}$ at different crystallization temperatures. The traces are vertically displaced for clarity. Melting point of slowly grown extended-chain crystals was determined as 129.5 °C.

capillary was fed through the VME interface and recorded together with X-ray detector time-frames. The ***q*** scale of the diffractograms was calibrated using wet rat tail collagen (low ***q*** range) and standard powder samples of a series of *n*-alkanes with ≤44 C atoms in the orthorhombic form (higher ***q*** range).

Results and Discussion

Isothermal Crystallization of $C_{294}H_{590}$. For the longest alkane in the present series, $C_{294}H_{590}$, isothermal crystallization exotherms were recorded by cooling the sample from 10 K above the extended chain melting point (see Table 1) to the predetermined crystallization temperature T_c. In order to prevent temperature undershot and to arrive at T_c with a nearly equilibrated instrument, T_c was approached in a sequence of ramps with decreasing cooling rates as follows: 50 °C/min to T_c + 10 °C, 20 °C/min to T_c + 5 °C, 10 °C/min to T_c + 2.5 °C, 5 °C/min to T_c + 1 °C, 2.5 °C/min to T_c + 0.5, and 1 °C/min to T_c. The approach to T_c was slower than in the case of $C_{246}H_{494}$,[6] since in the present case the crystallization times are considerably longer, in line with the steep reduction in measured growth rate with increasing chain length.[8] A series of representative crystallization exotherms of $C_{294}H_{590}$ are shown in Figure 1.

Starting with the T_c = 129.0 °C thermogram and moving to lower temperatures, the overall crystallization process is seen to accelerate at first, but then it levels off, and between 126 and 123.8 °C it actually slows down somewhat, judging by the small shift in position of the exothermic maximum toward longer times. At temperatures of 123.7 and 123.6 °C, multiple exotherms are resolved, a behavior similar to that of $C_{246}H_{494}$ around 121.0 °C.[6] At and below 123.4 °C there is only a single peak, which moves rapidly to shorter times as T_c is lowered further. From the similarity with the behavior of $C_{246}H_{494}$ we conclude that, above the temperature of the multiple exotherm, crystallization of $C_{294}H_{590}$, like that of $C_{246}H_{494}$, takes place in the extended chain form; analogously, at temperatures below the multiple exotherms, it occurs in the once-folded form. Supporting this interpretation are the independently measured melting points of alkanes $C_{246}H_{494}$ and $C_{294}H_{590}$ in the once-folded crystal form. These are, respectively, 122.5 ± 1.0 and 124.0 ± 0.5 °C.

A brief discussion of the transition temperature region and the shape of the exotherms is given separately further below.

Of our main current concern is the fact that the overall crystallization rate shows a small but significant slowdown as the temperature is decreased below 126 °C. While the thermograms in Figure 1 speak for themselves, in order to present the data in a quantitative form we choose the empirical rate parameter $1/t_{10\%}$ and plot it against T_c in Figure 2. $t_{10\%}$ represents the time required for crystallization to reach 10%, i.e. for the evolution of 10% of the total heat of crystallization. The same parameter has been used in the case of $C_{246}H_{494}$,[6] hence, the two datasets can be compared directly. $1/t_{10\%}$ is affected by both crystal nucleation and growth. However, separate measurements for $C_{246}H_{494}$ have shown[8] that the rates of both of these processes have similar temperature dependencies, both being reasonably well represented by $1/t_{10\%}$.

As seen in Figure 2 the crystallization rate parameter $1/t_{10\%}$ exhibits a shallow minimum as a function of crystallization temperature. While the minimum is not as pronounced as in the shorter alkanes $C_{246}H_{494}$ and $C_{198}H_{398}$, the rate of extended-chain crystallization near the extended-to-folded crystallization transition is still several times lower than the extrapolated rate based on the rate/temperature gradient at small ΔT. Whereas the presence of the anomalous retardation is unquestionable, the reason that it is less pronounced than in shorter alkanes is not known at present.

Nonisothermal Crystallization of $C_{258}H_{518}$ through $C_{194}H_{390}$. Isothermal crystallization experiments cannot be performed reliably by DSC when crystallization rates are high because of the finite time required for the equilibration of the instrument after reaching T_c. Since the overall gradient of rate *vs* supercooling is high for shorter chain alkanes, isothermal experiments could only be performed at the smallest ΔT. We thus had to resort to nonisothermal experiments in order to observe the rate minimum for alkanes in the region of 200 C atoms and shorter. These experiments were in fact straightforward cooling DSC scans through the crystallization temperature range carried out at a cooling rate appropriate to each particular alkane.

Cooling DSC thermograms for alkanes $C_{258}H_{518}$, $C_{246}H_{494}$, $C_{210}H_{422}$ and $C_{198}H_{398}$ are shown in Figure 3. The respective cooling rates were 0.4, 2, 30, and 40 °C/min. Under these conditions all four alkanes show two distinct exothermic maxima with a minimum in between them. The cooling scan for $C_{198}H_{398}$ had already been reported previously.[6] The key point to note here is that the area of the high-temperature exotherm is the smaller of the two. The minimum in heat evolution rate situated between the two peaks means therefore that the overall crystallization slows down already after only a minority of the sample had crystallized. Moreover, the retardation occurs in spite of the fact that the total number of crystals in existence could have only increased in the process, even if the nucleation *rate* decreased at the minimum. Thus the shapes of the thermograms in Figure 3 demonstrate clearly that all four alkanes show a *deep minimum in crystal growth rate*.

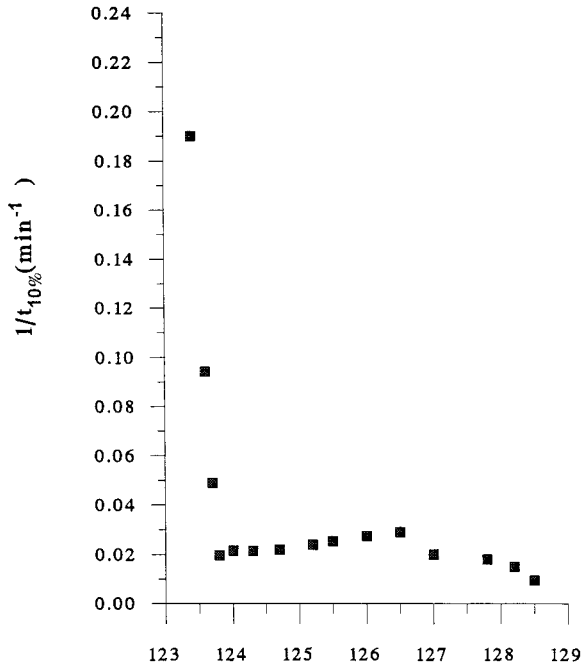

Figure 2. Empirical crystallization parameter $1/t_{10\%}$ as a function of crystallization temperature T_c for alkane $C_{294}H_{590}$. $t_{10\%}$ is the time elapsed between reaching T_c and the attainment of 10% of ultimate crystallinity.

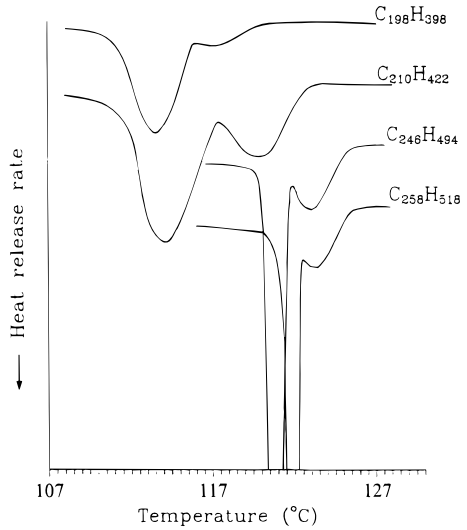

Figure 3. Cooling DSC thermograms for alkanes $C_{258}H_{518}$, $C_{246}H_{494}$, $C_{210}H_{422}$, and $C_{198}H_{398}$ recorded, respectively, at cooling rates of 0.4, 2, 30, and 40 °C/min.

The ratio of areas of the two exotherms could be varied by varying the cooling rate. The cooling rates in Figure 3 were chosen such that the area of the higher temperature peak is the smaller of the two, in order to clearly demonstrate that the minimum is the consequence of genuine retardation in crystallization and not of postcrystallization effects such as occur in the transition temperature region in the isothermal experiments (see next section). With the decrease in the cooling rate, the ratio of the areas changes in favor of the high-temperature exotherm, as the alkane has more time to crystallize in the extended-chain form above the growth rate minimum temperature T^*. With an increase in the cooling rate, the reverse happens.

The effect of cooling rate is illustrated in Figure 4 on the example of $C_{246}H_{494}$. While at the slowest cooling rate of 0.5 °C/min almost all crystallization is contained in the higher temperature, i.e., extended-chain exotherm, at 2 °C/min most crystallization is in the folded-chain form, judging by the fact that the low-temperature exotherm is dominant. In order to confirm this assignment of the two exotherms, real time SAXS experiments were performed during continuous cooling of *n*-$C_{246}H_{494}$ from the melt at cooling rates 0.5 and 1 °C/min. The respective series of diffractograms are shown in Figure 5a,b. As seen in Figure 5a, cooling at 0.5 °C/min produces a series of diffraction orders (three shown in the figure) of the 259−260 Å periodicity, which is characteristic of extended $C_{246}H_{494}$ chains tilted at 35° to the layer normal (calculated periodicity: $(246 \times 1.27 + 2)(\cos 35°) = 258$ Å.[11] The angle of 35° is the tilt of the {201} crystallographic basal planes, and is common in the high temperature form of long alkanes,[12] as well as in some shorter *n*-alkanes,[13] and in chain-folded polyethylene.[14a] In the 0.5 °C/min cooling run a small diffraction peak at 201 Å develops at lower temperatures. This corresponds to the non-integer folded (NIF) form.[12] It should be noted that the structure factor and hence intrinsic diffraction intensity of the first-order NIF reflection is significantly higher than those of any of the extended-chain reflections; therefore, the impression of the extent of chain-folded crystallization is exaggerated in Figure 5a.

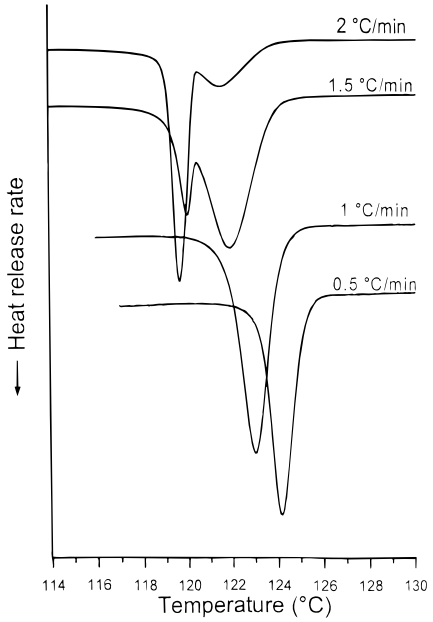

Figure 4. Cooling thermograms of alkane $C_{246}H_{494}$ recorded at cooling rates of 0.5, 1, 1.5, and 2 °C/min.

In Figure 5b the series of SAXS diffractograms recorded during a 1 °C/min cooling sequence shows that the crystallization in the NIF form is dominant: two orders are seen of a periodicity which starts at around 200 Å and gradually decreases to 170 Å with decreasing temperature. However, at the beginning of the run, starting at 123 °C, weak diffraction from extended-chain crystals appear (two orders). As in the 0.5 °C/min sequence (Figure 5a), the actual ratio of extended- to folded-chain crystallization is higher then suggested by the relative diffraction intensities of the two forms. Even so, it is clear that, while the 1 °C/min SAXS experiment in Figure 5b shows chain-folded crystallization, only a single exotherm associated with extended-chain crystallization is observed in the equivalent DSC run.

The above systematic difference between the SAXS and the DSC experiments in Figures 4 and 5 is consistent with the previous observation[6] that nucle-

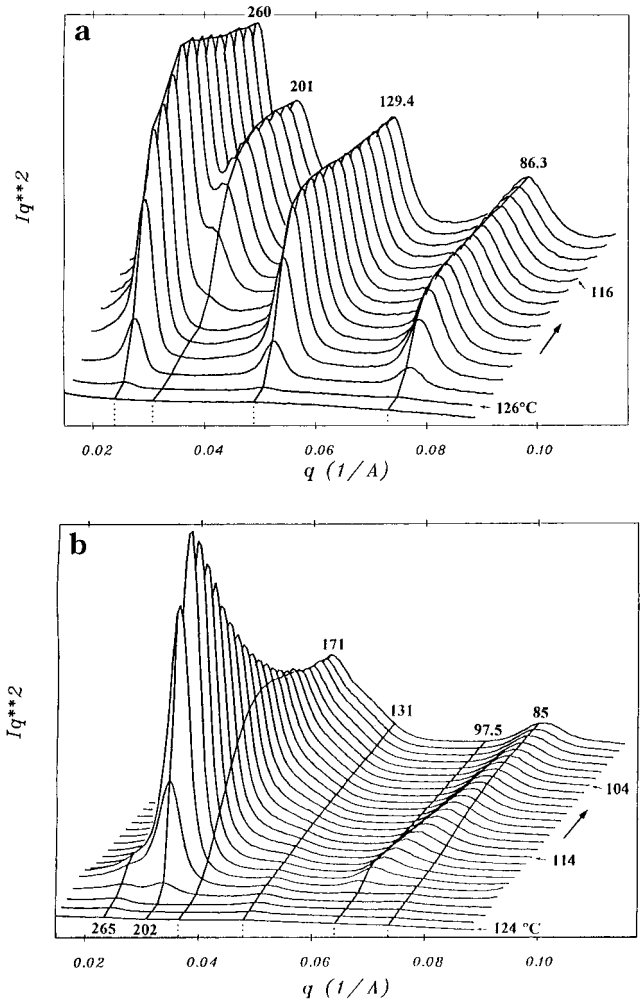

Figure 5. Real time SAXS curves recorded during cooling of alkane $C_{246}H_{494}$ at 0.5 (a) and 1 °C/min (b). Each frame covers a 1 °C interval. Intensities are Lorentz corrected. d-spacings corresponding to constant q lines ($d = 2\pi/q$) are indicated in Å. Temperatures are indicated on the right. In part a, three diffraction orders of tilted extended-chain crystals are seen (260, 129.4, and 86.3 Å) as well as the first-order NIF reflection (201 Å). In part b two diffraction orders of NIF are dominant, with two weak reflections from extended chains (265 and 131Å).

ation in the DSC experiment is generally faster than in the X-ray experiment, a phenomenon probably related to surface nucleation on container walls (aluminium *vs* glass); hence, in a DSC experiment a higher proportion of the material succeeds in crystallizing in the extended-chain form, compared with the SAXS experiment at the same cooling rate. This difference appears consistently in our experiments, also involving other alkanes. Once this difference in nucleation rate is taken into account, the real-time SAXS experiment agrees well with the assignment of two exotherms in the cooling DSC scans.

For the shortest alkane in this study, $C_{194}H_{390}$, a DSC cooling rate could not be achieved which would be high enough to maintain the high-temperature exotherm as a minority component. Figure 6 shows the thermogram of $C_{194}H_{390}$ recorded with a cooling rate of 40 °C/min. The doublet is still observed, but the ratio of the areas is reversed compared to that of the next nearest alkane $C_{198}H_{398}$.

Shape of Isothermal Crystallization Exotherms in $C_{294}H_{590}$. We now return to the question of the origin of the multiple exotherm in isothermal crystallization

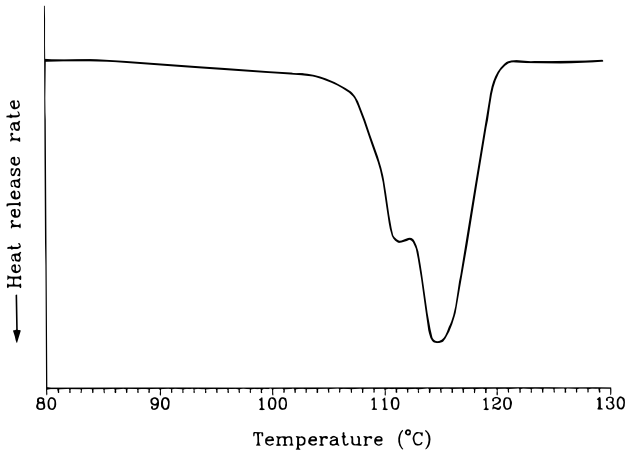

Figure 6. Cooling DSC thermogram of $C_{194}H_{390}$ recorded at 40 °C/min.

of $C_{294}H_{590}$ at 123.7 and 123.6 °C. It was shown for $C_{246}H_{494}$ by real-time SAXS[6] that in the region of the multiple exotherm the first crystals to appear are chain-folded, or more precisely, noninteger folded (NIF); this is followed by their disappearance through isothermal thickening, so that subsequent crystallization takes place directly in the extended-chain form on the already existing extended-chain substrate. In $C_{246}H_{494}$ only two and not three exothermic maxima were observed in the transition region. The first was unequivocally associated with folded-chain nucleation and growth. In order to explain the appearance of the second exotherm, it was proposed that once extended chain crystals appear through thickening, they trigger the comparatively rapid chain-extended growth. This shows up in two ways: if thickening occurs after the bulk of the crystallization is over, an additional exotherm appears at the tail end of the main chain-folded crystallization exotherm (see 123.7 and 123.6 °C traces in Figure 1). If thickening happens before the crystallization of the bulk, then only a single exotherm is observed. This may have a shoulder at its front end, as in the case of $C_{246}H_{494}$ crystallization at 121.1 °C,[6] or only a somewhat extended leading portion, as in the present case of $C_{294}H_{590}$ at 123.8 °C. While a small amount of early crystallization may be occurring in the folded-chain form at 123.8 °C, only extended-chain crystallization is expected at higher temperatures, in view of the steep temperature gradient of the rate of folded-chain crystallization (Figure 2).

The acceleration in crystallization upon folded-chain to extended-chain crystal transformation, indicated by both the present and the previous results,[6] has significant implications for the crystallization theory. The inference is that for extended chains crystal *growth* is faster, while *nucleation* is slower, than the respective rates for folded chains. However, this directly contravenes the prediction of the polymer nucleation theory,[14b,15,16] which states that the critical fold length l of a primary nucleus is always larger than that of a secondary nucleus (crystal growth); in the case of homogeneous nucleation the predicted ratio is 2:1.

At this time we do not have sufficient data to understand the detailed shape of the thermograms, but we expect more information from new real-time combined small- and wide-angle X-ray experiments planned in the future. Thus we leave unanswered the question of the origin of the third exotherm in the 123.7 °C thermogram. Suffice it to say that it is not inconceivable

that in a narrow transition temperature range where folded- and extended-chain nucleation rates are similar, two parallel and independent processes may take place. The first, nucleation/growth of folded-chain crystals, and the second, nucleation/growth of extended-chain crystals, would produce two exothermic peaks if their bulk crystallization rate maxima do not coincide in time. One possibility is that these two processes account for the first and the second exotherm, with the small third exotherm being triggered by chain extension of the folded-chain crystals. For the time being, however, this interpretation remains only a speculation.

Conclusion

In summary, the present study has confirmed the existence of a minimum in bulk crystallization rate *vs* temperature for six monodisperse *n*-alkanes ranging between 194 and 294 C atoms in length. The effect, previously observed for two alkanes, $C_{246}H_{494}$ and $C_{198}H_{398}$,[6,7] can therefore be regarded as being of wider generality, at least in the case of *n*-alkanes. The anomalous retardation of the growth rate of extended-chain crystals in the vicinity of the folded chain crystal melting point has been interpreted in terms of surface "self-poisoning", i.e. obstruction to chain extension by frequent deposition of nearly-stable chain-folded overgrowth.[4,6] Simple rate equation models based on this hypothesis,[17,18] as well as computer simulation,[18] were able to reproduce the qualitative features of the experimental rate curves with remarkable success. An alternative interpretation, in terms of the secondary nucleation theory, has also been proposed.[19] Further experimental and simulation studies are in progress.

Note Added in Proof

Since the submission of this article Sutton *et al.* also reported the observation of the crystal growth rate minimum for *n*-$C_{294}H_{590}$.[20]

Acknowledgment. Financial support from the Engineering and Physical Science Research Council is gratefully acknowledged. E.B. wishes to thank the University of Sheffield for her Research Scholarship. We thank Drs. E. Komanschek and S. Slawson for help and advice with synchrotron experiments.

References and Notes

(1) Bidd, I.; Whiting, M. C. *J. Chem. Soc., Chem Commun.* **1985**, 543. Bidd, I.; Holdup, D. W.; Whiting, M. C. *J. Chem. Soc., Perkin Trans. 1* **1987**, 2455.
(2) Lee, K. S.; Wegner, G. *Makromol. Chem., Rapid Commun.* **1985**, *6*, 203.
(3) Ungar, G.; Stejny, J.; Keller, A.; Bidd, I.; Whiting, M. C. *Science* **1985**, *229*, 386.
(4) Ungar, G. In *Integration of Fundamental Polymer Science and Technology*, Lemstra, P. J., Kleintjens, I. A., Eds.; Elsevier Appl. Sci.: Oxford, U.K., 1988; Vol. 2, pp 346−362.
(5) Alamo, R. G. In *Crystallization of Polymers*; NATO ASI Series C405, Dosiere, M., Ed.; Kluwer: Dordrecht, The Netherlands, 1993; pp 73−80.
(6) Ungar, G.; Keller, A. *Polymer* **1987**, *28*, 1899.
(7) Organ, S. J.; Ungar, G.; Keller, A. *Macromolecules* **1989**, *22*, 1995.
(8) Organ, S. J.; Ungar, G.; Keller, A.; Hikosaka, M. *Polymer* **1996**, *37*, 2517.
(9) Alamo, R. G.; Mandelkern, L.; Stack, G. M.; Krohnke, C.; Wegner, G. *Macromolecules* **1994**, *27*, 147.
(10) Brooke, G. M.; Burnett, S.; Mohammed, S.; Proctor, D.; Whiting, M. C. *J. Chem. Soc., Perkin Trans. 1*, **1996**, 1635.
(11) Broadhurst, M. G. *J. Res. Natl. Bur. Stand., Sect. A* **1962**, *66*, 241.
(12) Ungar, G.; Keller, A. *Polymer* **1986**, *27*, 1835.
(13) Takamizawa, K.; Ogawa, Y.; Oyama, T. *Polym. J.* **1982**, *14*, 441.
(14) (a) Wunderlich, B. *Macromolecular Physics*; Academic Press: New York: 1974, Vol 1; (b) 1976, Vol. 2.
(15) Turnbull, D.; Fischer, J. C. *J. Chem. Phys.* **1949**, *17*, 71.
(16) Hoffman, J. D.; Davis, G. T.; Lauritzen, J. I., Jr. In *Treatise in Solid State Chemistry*, Hannay, N. B., Ed.; Plenum Press: New York, 1976; p 497.
(17) Sadler, D. M.; Gilmer, G. H. *Polym. Commun.* **1987**, *28*, 243.
(18) Higgs, P. G.; Ungar, G. *J. Chem. Phys.* **1994**, *100*, 640.
(19) Hoffman, J. D. *Polymer* **1992**, *32*, 2828.
(20) Sutton, S. J.; Vaughan, A. S.; Bassett, D. C. *Polymer* **1996**, *25*, 5735.

MA961599J